Monitoring of ducting by using a ground-based GPS receiver*

Sheng Zheng(盛 峥)[a)b)] and Fang Han-Xian(方涵先)[a)†]

[a)] College of Meteorology and Oceangraphy, PLA University of Science and Technology, Nanjing 211101, China
[b)] Sate Key Laboratory of Space Weather, Chinese Academy of Sciences, Beijing 100190, China

(Received 29 March 2012; revised manuscript received 2 July 2012)

In this paper, we describe the estimation of low-altitude refractivity structure from simulation and real ground-based GPS delays. The vertical structure of the refractive environment is modeled using three parameters, i.e., duct height, duct thickness, and duct slope. The refractivity model is implemented with a priori constraints on the duct height, thickness, and strength, which might be derived from soundings or numerical weather-prediction models. A ray propagation model maps the refractivity structure into a replica field. Replica fields are compared with the simulation observed data using a squared-error objective function. A global search for the three environmental parameters is performed using a genetic algorithm. The inversion is assessed by comparing the refractivity profiles from the radiosondes to those estimated. This technique could provide near-real-time estimation of the ducting effect. The results suggest that ground-based GPS provides significant atmospheric refractivity information, despite certain fundamental limitations of ground-based measurements. Radiosondes are typically launched just a few times daily. Consequently, estimates of temporally and spatially varying refractivity that assimilate GPS delays could substantially improve over-estimates caused by using radiosonde data alone.

Keywords: global positioning system, ducting, genetic algorithm, radio remote sensing

PACS: 93.85.Ly, 41.20.Jb **DOI:** 10.1088/1674-1056/22/2/029301

1. Introduction

Historically, the vertical profile of the atmospheric refractivity of a "standard atmosphere" has been used as a basis for wireless system performance predictions.[1,2] Since the mid-1980s it has become common practice to improve this profile with surface observations of air temperature, sea temperature, wind speed, and relative humidity, in conjunction with an atmospheric surface-layer model to estimate the refractivity profile within the marine atmospheric surface layer. The refractivity profile above the surface layer is not characterized by the surface layer models but usually determined by weather balloons or radiosondes. However, whereas the surface layer measurements can be made continuously, weather balloons or rocket soundings are expensive in terms of expendables and manpower.[3] An alternative means for estimating refractivity is to use ground-based GPS.[4]

Terrestrial propagation of radio waves at frequencies above 30 MHz is significantly affected by tropospheric refraction, especially when the source and/or receiver is near a coastline. Knowledge of the refractive environment is crucially important to predict radar detection ranges or maximum microwave communication ranges. However, radiosonde measurements are expensive, and they may undersample the spatial and temporal variations in refractory phenomena, particularly near coastlines. Ground-based measurements are potentially more informative about space–time variations of refractivity in a particular region, but analyses of ground-based sensing of atmospheric refractivity thus far have examined that potential largely on the basis of simulated observations. Applications of ground-based refractivity profiling are comparatively few, and profiling from GPS measurements has not yet been documented, primarily because of an inherent limitation of the source–receiver geometry. Ground-based refractivity profiling is further hampered by the need to develop instruments and algorithms that can accurately measure signal delay at the low satellite elevation angles ($< 5^\circ$) that convey most of the refractive information.[5]

2. Ducting

Ducting is caused by a strong gradient in refractivity N in altitude.[6] According to Smith and Weintraub law, refractivity itself can be expressed as

$$N_i = 77.6\frac{P_i}{T_i} + 3.73\times 10^5 \frac{e_i}{T_i^2}, \tag{1}$$

where P_i and e_i are the atmospheric pressure and water vapour partial pressure at level i in hectopascals, T_i is the atmospheric temperature at level i in Kelvin.

The refractivity gradient $\mathrm{d}N/\mathrm{d}r$ is used to characterize the atmospheric conditions with respect to altitude r. If a region has a positive gradient, the region is called a subrefractive region. In these subrefractive regions, radio waves are

*Project supported by the National Natural Science Foundation of China (Grant No. 41105013), the National Natural Science Foundation of Jiangsu Province, China (Grant No. BK2011122), the Specialized Research Fund for State Key Laboratories, China (Grant No. 201120FSIC-03), and the City Meteorological Scientific Research Fund, China (Grant No. IUMKY&UMRF201111).

†Corresponding author. E-mail: 19994035@sina.com

© 2013 Chinese Physical Society and IOP Publishing Ltd

refracted away from Earth's surface. Regions with the gradient between $-76\ \mathrm{N{\cdot}km^{-1}}$ and $0\ \mathrm{N{\cdot}km^{-1}}$ are normal refraction regions. Regions with $\mathrm{d}N/\mathrm{d}r$ between $-76\ \mathrm{N{\cdot}km^{-1}}$ and about $-160\ \mathrm{N{\cdot}km^{-1}}$ are called super-refractive regions. When the radius of curvature of the ray is equal to the radius of curvature of the atmosphere, the ray will propagate at a fixed height above the surface and the region is critical refraction region. Ducts appear when $\mathrm{d}N/\mathrm{d}r$ leads to rays that curve down into the surface at low altitudes, which can be expressed as

$$\frac{\mathrm{d}N}{\mathrm{d}r} \leq \frac{-10^6}{R_\mathrm{c}}, \tag{2}$$

where R_c is the radius of curvature of the atmosphere in km. When $\mathrm{d}N/\mathrm{d}r$ is less than $-160\ \mathrm{km^{-1}}$ for a mean value of R_c, this condition occurs.

Performing the derivative $\mathrm{d}N/\mathrm{d}r = N'$ results in four contributing terms, equation (3) can be obtained as

$$\begin{aligned} N' \ =\ & 77.6\cdot P'\cdot\frac{1}{T} - 77.6\cdot T'\cdot\frac{p}{T^2} \\ & + 3.73\times 10^5\cdot e'\cdot\frac{1}{T^2} - 3.73\times 10^5\cdot T'\cdot\frac{e}{T^3}. \end{aligned} \tag{3}$$

The first term represents the hydrostatic variations of pressure with altitude, it is about $-30\ \mathrm{km^{-1}}$ in the lowest few kilometers of the atmosphere. The second term may be closer to the ground surface where higher pressure is found. The third term will generally contribute to ducting at altitudes where strong gradients in humidity pressure are found. The fourth term is negligible.

Ducting has been observed in radiosonde data up to about 4 km in altitude, but most ducting events are found below 2 km.[7]

3. Excess phase path model

Assuming the atmosphere to be spherically and radially symmetric refractive medium, GPS excess phase path is modeled using an integral expression derived from Snell's law $\mu r\sin\alpha = a$, where r is the local radius of curvature of the ray, μ is the refractive index, α is the zenith angle of the ray, and a is the constant impact parameter.

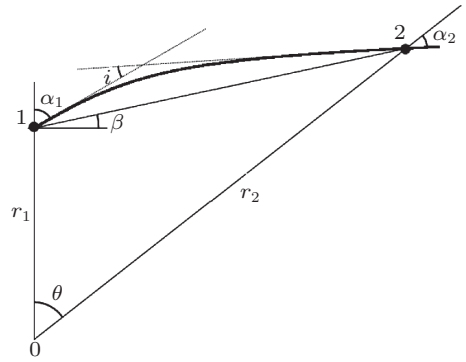


Fig. 1. Schematic diagram of the geometric parameters for refractive bending.

The GPS excess phase path is modeled using an integral expression derived from ray theory.[8] Assuming a spherically, radially symmetric refractive medium, a ray is described by Snell's law (Fig. 1).

The phase path between points 1 and 2 on a ray is

$$S = \int_1^2 n(r)\,\mathrm{d}l, \tag{4}$$

where $\mathrm{d}l$ can be written as $\mathrm{d}l = \sqrt{\mathrm{d}r^2 + r^2\mathrm{d}\theta^2}$ in polar coordinates. Substituting $\mathrm{d}r = \mathrm{d}l\cos\alpha$ and using Snell's law, equation (4) may be expressed as

$$S = \int_{r_1}^{r_2} \frac{rn^2(r)}{\sqrt{rn^2(r)-a^2}}\,\mathrm{d}r = \int_{x_1}^{x_2} \frac{\left[1-\dfrac{x}{n}\dfrac{\mathrm{d}n}{\mathrm{d}x}\right]}{\sqrt{x^2-a^2}}\,\mathrm{d}x. \tag{5}$$

Here, $x \equiv rn(r)$ is the refractional radius. Equation (5) permits the calculation of the phase path S for a given impact parameter or for given zenith angle of the ray at a point. The excess phase path is simply $DS = S - S_0$ (where S_0 is the path in vacuum, i.e., the geometrical distance between the antenna 1 and GPS satellite 2) and is a function of the elevation angle β of the straight line connecting antenna 1 and GPS satellite 2. Excess phase path DS cannot be calculated explicitly for given β; rather, we calculate DS and β for a given impact parameter a using the bending angle i of the ray connecting satellite and receiver

$$i = \int_1^2 \frac{\mathrm{d}l}{\rho}, \tag{6}$$

where r is the local radius of curvature of the ray, and $r' = \mathrm{d}r/\mathrm{d}\theta$. In polar coordinates

$$\rho = \frac{[r^2 + (r')^2]^{3/2}}{r^2 + 2(r')^2 - r(r'')}. \tag{7}$$

Substituting expression (7) into expression (6) and using Snell's law (1), the expression for i is

$$\begin{aligned} i \ &= -a\int_{r_1}^{r_2} \frac{\mathrm{d}n/\mathrm{d}r}{n(r)\sqrt{r^2n^2(r)-a^2}}\,\mathrm{d}r \\ &= -a\int_{x_1}^{x_2} \frac{\mathrm{d}n/\mathrm{d}r}{n(x)\sqrt{x^2-a^2}}\,\mathrm{d}x. \end{aligned} \tag{8}$$

Once S and ε are calculated, the spherical angle θ between points 1 and 2 can be obtained, and the elevation angle β is then

$$\beta = \arctan\left(\frac{r_2\cos\theta - r_1}{r_2\sin\theta}\right), \tag{9}$$

and the path in vacuum S_0 is

$$S_0 = \sqrt{r_1^2 + r_2^2 - 2r_1r_2\cos\theta}. \tag{10}$$

Finally, we can obtain the excess phase path from $DS(\beta) = S - S_0$.

4. Parameter search for best fit model

In order to parameterize the refractivity structure, a three-parameter refractivity model is designed to describe the refractivity structure. Each modeled excess phase path $DS^{\mathrm{mod}}(\beta)$ is calculated, and compared with the GPS measurement of excess phase path $DS^{\mathrm{GPS}}(\beta)$ to determine which provides the best fit in a least squares sense.

4.1. Refractivity parameters model

The model design is motivated partly by a desire to characterize anomalous refractivity gradients, and it can be seen from Fig. 2. Normally, the vertical refractivity gradient is negative, i.e., $\mathrm{d}N/\mathrm{d}r < 0$, so that rays are bent toward the Earth's surface, and most often the radius of curvature of rays is greater than the Earth's radius r_E. However, when the radius of ray curvature at a tangent point is equal to the spherical radius, i.e., $\mathrm{d}N/\mathrm{d}r = -n/r \approx -160\ \mathrm{N{\cdot}km^{-1}}$, the ray is critically refracted, and when $\mathrm{d}N/\mathrm{d}r < -n/r$, it is referred to as superrefraction. Rays having tangent points within a superrefracting layer are trapped.

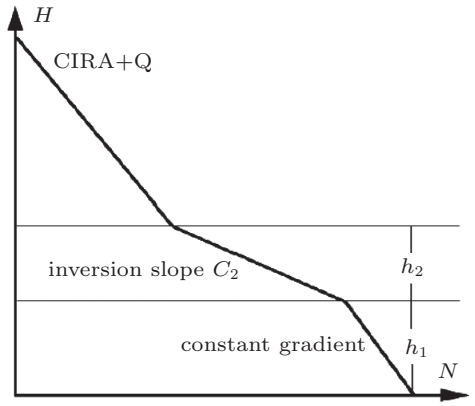


Fig. 2. Refractivity model using three parameters.

The refractivity model used here consists of a constant gradient (40 $\mathrm{N{\cdot}km^{-1}}$) beginning at the receiver altitude and h_1, a critically refractive gradient c_2 (more than 160 $\mathrm{N{\cdot}km^{-1}}$) between altitudes h_1 and $h_1 + h_2$, and the gradient between $h_1 + h_2$ and 6 km altitude can be obtained from CIRA+Q model. There are only three independent variable parameters in the model, corresponding to the altitudes h_1, h_2, and the critically refractive gradient c_2. Refractivity at the receiver N_1, is calculated from pressure, temperature, and relative humidity (P, T, e) collected at the surface meteorological sensor.

4.2. Search bounds for parameters

To determine the "best fit" model of ΔS^{GPS}, we perform the genetic algorithm (GA) to search the best parameters.[9,10] The set of parameters described in Subsection 4.1 was used in the optimization. The parameters and their search bounds are given in Table 1. In actual implementations, prior information might be available from a variety of sources (e.g., numerical weather prediction models, atmospheric soundings, etc.) that could improve the quality of the inverse problem solutions.[11]

Table 1. Parameter search bounds for the refractivity model.

Parameter	Lower bound	Upper bound
Base height h_1	0	1500
Inversion thickness h_2	0	500
Inversion slope c_2	–0.6	0.3

It is assumed that the difference (m) between the simulated observed $DS^{\mathrm{GPS}}(\beta)$ and modeled $DS^{\mathrm{mod}}(\beta)$ clutter is Gaussian, $\Delta S^{\mathrm{GPS}} = DS^{\mathrm{GPS}}(\beta) - DS^{\mathrm{mod}}(\beta)$. This leads to a simple least squares objective function:

$$\phi(\beta) = \Delta S^{\mathrm{GPS^T}} \cdot \Delta S^{\mathrm{GPS}}. \tag{11}$$

The simulated GA code is used to optimize Eq. (11). The GA-search parameters are parameter quantization 256 values; population size 32; reproduction size 0.5; cross-over probability 0.1; the number of iterations for each population 100; and the number of populations 50. Thus 5000 forward modeling runs are performed for each inversion.

5. Results using ground-based GPS data

In order to test the proposed refractivity estimation method, simulation and real ground-based GPS were used. Simulated data were generated using a known radiosonde refractivity profile, and then simulated excess phase path can be obtained. The simulated excess phase path was used as observation data to estimate refractivity model, and the refractivity model that best fit the GPS excess phase path ΔS^{GPS} were compared with the refractivity structure measured by radiosondes. Four high-resolution Vaisala radiosondes ($\sim$ 20 m sampling at altitudes $<$ 6 km) were released from the instrument pier on Helena (15.94 S, 5.67 W).

True ground-based GPS observation data from the observation in Jiangxi Poyang lake (115.27 E, 29.11 N), the corresponding sounding data from the meteorological rocket detection data ($\sim$ 4 m sampling at altitudes $<$ 1.5 km) and low-resolution radiosondes ($\sim$ 50 m sampling at altitudes $<$ 6 km) were obtained, and observation time was 17 April 2009, and there were two observations in total. GPS observation data were disposed by another pibal factory, and its primary purpose was to estimate spatial wind field. Accidental product included GPS excess phase path delays, and then the delays could be used to estimate refractivity structure.

5.1. Ground-based GPS data processing

GPS data are collected from SNR receiver with benchmark ACT tracking. All data are collected into a single personal computer. The observable we used to retrieve refractivity is the excess phase path, i.e., the excess travel time between

satellite and receiver which results from tropospheric bending and slowing, multiplied by the speed of light in vacuum. GPS excess phase path is estimated using a modified version of Bernese v5.0 software in a precise point positioning mode.[12] Accurate point positioning requires precise ephemerides and satellite clock estimates, the Jet Propulsion Laboratory (JPL) or GFZ orbits are used. Because the GPS data were sampled at 1 Hz rate, the 1/30 Hz satellite clock is derived by interpolation.

In order to obtain excess phase path, there are three parameters that need to be estimated when processing the carrier phase and code GPS observation. The first item is the receiver clock error at each epoch, the second item is the phase ambiguity, and the third item is tropospheric wet zenith delay at half-hourly intervals. Tropospheric dry delay and wet delay are modeled by Niell's mapping function. Ionospheric dispersive delay is removed using the ionosphere-free linear combination of phases from the two GPS carrier frequencies. The information that is retained after Bernese processing included (i) the position of the receiver, (ii) the position and velocity of the GPS satellite derived from the precise ephemerides, and (iii) the measured excess phase path.

The measured excess phase path ΔS^{GPS} varies from about 2 m at zenith to more than 100 m at low satellite elevation angles. Lowest elevation data are prone to gaps in observations, partly because of masking by structures and topography east of the instrument and partly because of multipath cancellation. Reflections off the lake surface generate strong multipath, and signal strength reduction by destructive interference commonly results in loss of L2 phase lock for satellites at low elevation. So in order to ensure the accuracy of measured excess phase path ΔS^{GPS}, the ΔS^{GPS} must vary smooth along with satellite elevation angles, and the best satellite elevation angle is about 1°, corresponding excess phase path ΔS^{GPS} is about 60 m–70 m.

5.2. Estimated accuracy using simulated ground-based GPS data

Figure 3 depicts modeling of ΔS^{GPS} measurements coincident with the four radiosondes launched from the instrument platform at Point Helena (Fig. 3(a): 0701211, Fig. 3(b): 01050211, Fig. 3(c): 01070211, and Fig. 3(d): 01070311). Best fit models of ΔS^{GPS} are shown as solid black lines. The radiosonde refractivity (depicted as black dash lines) generally coincides with low RMS misfit $\left\| DS^{\mathrm{GPS}}(\beta) - DS^{\mathrm{mod}}(\beta) \right\|$. Moreover, in most cases (i.e., Figs. 3(a)–3(c)) the model that best fits ΔS^{GPS} closely approximates the model that would best fit the radiosonde refractivity.

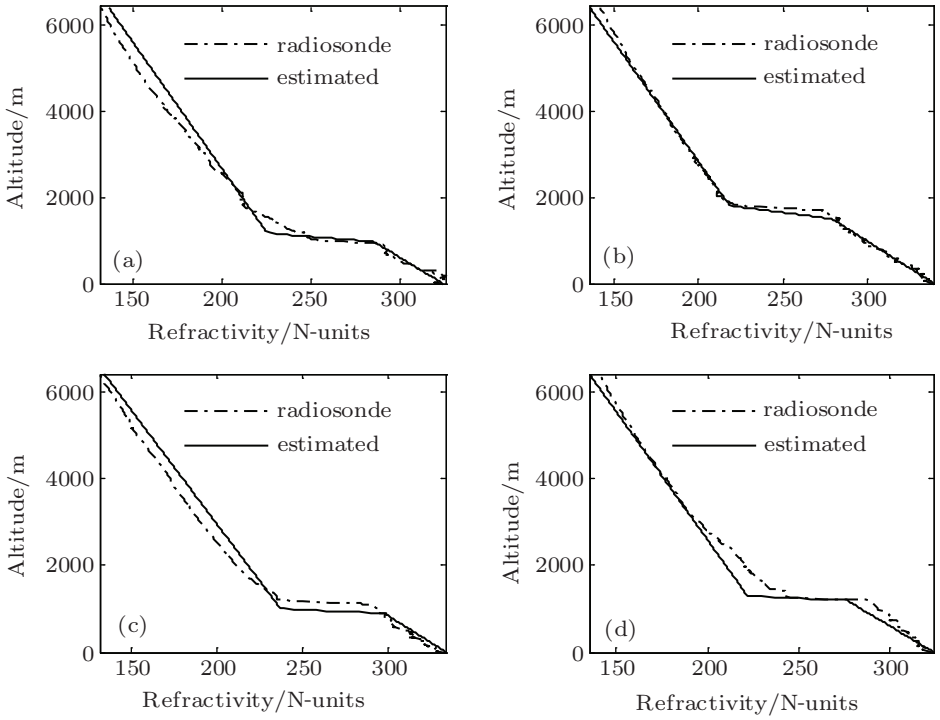


Fig. 3. Curves of refractivity versus altitude for the four radiosondes released from the instrument pier at Point Helena. Dashed lines represent radiosonde measurements, and solid black lines denote the results from the best fit model of ΔS^{GPS}.

The refractivity model that best fits ΔS^{GPS} does not always match the radiosonde refractivity profile, however. In Fig. 3(d) the best fitting model has a large ($\sim$ 30 N-unit lapse) duct beginning at 1200-m altitude. The radiosonde refractivity gradient is more variable than in other examples, but a model having a smaller duct at lower altitude would better match the observed radiosonde refractivity. The difference between radiosonde and GPS estimates of refractivity in Fig. 3(d) sim-

ply demonstrates that ground-based measurements of excess phase path do not always adequately constrain the altitude of anomalous refractive structures. Poor constraint of altitude is a manifestation of the ill-posed nature of the integral equation.[13,14]

5.3. Estimated accuracy using real ground-based GPS data

Figure 4 depicts the excess phase paths with respect to GPS receiver elevation angle for two real data in Poyang lake, China (Fig. 4(a): time for 11:23 AM, and Fig. 4(b): time for 13:54 PM).

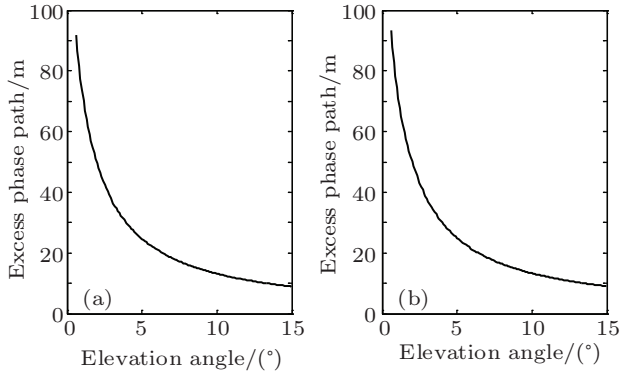


Fig. 4. Excess phase paths versus GPS receiver elevation angle.

Figure 5 depicts the estimated result using real ΔS^{GPS} measurements coincident with the two real data in the Poyang lake, China (Fig. 5(a): time for 11:23 AM, Fig. 5(b): time for 13:54 PM). Best fit models of ΔS^{GPS} are shown as solid black lines. The radiosonde refractivity (depicted as black dash lines) generally coincides with low RMS misfit $\left\| DS^{\mathrm{GPS}}(\beta) - DS^{\mathrm{mod}}(\beta) \right\|$.

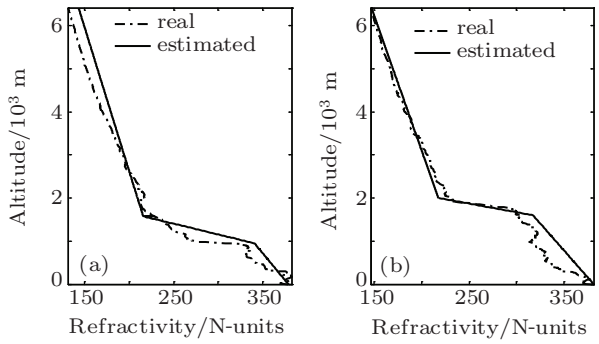


Fig. 5. Curves of refractivity versus altitude for the two real data from the instrument at Poyang lake of Jiangxi Province, China (Figs. 5(a) and Fig. 5(b)). Dashed lines represent real measurements, and solid black lines denote the results from the best fit model of ΔS^{GPS}.

It is shown in Fig. 5, when real ground-based GPS data are used, because real data have some observation errors, inversion accuracy is lower than that of simulated data. Since the foundation of the parameters of the model and GPS observations has defects, inversion result is too smooth and has a certain deviation between real sounding data, and vertical variation of depicting ability is bad. Overall, the inversion is successful if all the inversion results are considered, because the refractivity structure and characteristics are manifested well. Because there are only two groups ground-based GPS data, only a simple error and statistical analysis are discussed, the inverse average deviation error is 9.1 N, and RMS error is 10.5 N.

6. Discussion and conclusions

Remote sensing of atmospheric refractivity structure using ground-based GPS introduces a new technique to obtain a lower atmospheric refractivity profile, which has a large number of potential applications in communication and weather prediction.[15] Relatively poor constraint of the altitude of refractivity structures would restrict the utility of GPS for some purposes. Poor altitude resolution is an unavoidable consequence of the GPS receiver geometry and will not be easily overcome when the GPS receiver is on the ground. There is some other observation information such as Doppler shift that has less information content than the excess phase path used for this analysis, and while GPS waveform or amplitude data may offer additional observation information for estimating the vertical refractivity structure, it will require significant adaptation of existing instrumentation before being useful. Ultimately, the best way to solve the limited altitude resolution of ground-based GPS is to use crossing rays from multiple sites in a tomographic approach. In the future, incorporating the ground-based GPS observation data into a weather numerical prediction model will be a key consideration of our work.

References

[1] Yan H J 1996 *AJ* **112** 1312
[2] Wei M, Qin X, Wang X H and Jiang W M 2007 *Trans. Atmos. Sci.* **30** 736 (in Chinese)
[3] Sylvester J J, Konstanzer G C, Rottier J R, Dockery G D and Rowland J R 2001 *APL Tech. Dig.* **22** 473
[4] Lowry A R, Rocken C and Sokolovskiy S V 2002 *Radio Sci.* **37** 1041
[5] Sokolovskiy S V, Rocken C and Lowry A R 2001 *Radio Sci.* **36** 473
[6] Engeln A V and Teixeira J 2004 *J. Geophys. Res.* **109** 8104
[7] Rocken C 1997 *J. Geophys. Res.* **102** 849
[8] Wu Y Y, Hong Z J, Guo P and Zheng J 2010 *Chin. J. Geophys.* **53** 639
[9] Gerstoft P, Rogers L T, Krolik J K and Hodgkiss S W 2003 *Radio Sci.* **38** 8053
[10] Gerstoft P, Hodgkiss S W , Rogers L T and Jablecki M 2004 *Radio Sci.* **39** 6006
[11] Goldberg D E 1989 *Genetic Algorithms in Search, Optimization and Machine Learning* (Boston: Addison-Wesley Publishing Co.)
[12] Huang S X and Sheng Z 2006 *Acta Phys. Sin.* **55** 6720 (in Chinese)
[13] Sheng Z 2011 *Acta Phys. Sin.* **60** 119301 (in Chinese)
[14] Sheng Z and Fang H X 2012 *Chin. Phys.* B **21** 029301
[15] Guo P, Kuo Y H and Sokolovskiy S V 2011 *J. Atmos. Sci.* **68** 1703